20-JESTIE-0175 10.1109/JESTIE.2021.3066897

Regenerative Passive Snubber Circuit for High-Frequency Link Converters

Andrei Blinov, Senior Member, IEEE, Ievgen Verbytskyi, Member, IEEE,
Dimosthenis Peftitsis, Senior Member, IEEE and Dmitri Vinnikov, Senior Member, IEEE

***Abstract*- This letter presents a passive snubber circuit for high-frequency link cycloconverters, which typically suffer from voltage oscillations across matrix-stage semiconductor devices. The proposed passive snubber allows for effective damping of the oscillations and reduction of the peak voltage stress. It is based on an auxiliary transformer and a diode bridge rectifier, which are rated only for a fraction of total converter power regenerated back to the input DC source. The performance of the circuit was verified with 350 VDC/230 VAC, 1 kW SiC MOSFET-based experimental prototype and a reduction of the peak voltage overshoot from 2.24 to 1.55 times the nominal was achieved, without negative impact on the converter overall efficiency. As a result, the blocking voltage rating of the matrix-stage semiconductors can be reduced from 900 to 650 V.**

Index Terms—DC-AC power conversion, snubbers, MOSFETs, power transistors, pulse width modulated inverters[1]

I. Introduction

POWER electronic converters are widely used to interface different DC sources into the AC grid [1]. Depending on the application requirements, non-isolated or isolated systems can be used. The latter are generally more complex and usually utilize two-stage conversion with an intermediate DC link [2]. Alternatively, a range of single-stage solutions has been proposed that can be referred to as high-frequency-link converters (HFLCs), cycloconverters or isolated matrix converters [3] (Fig. 1). Such topologies have been proposed for battery, renewable, traction and DC microgrid applications. The potential advantages include absence of a DC-link capacitor and soft switching operation of semiconductors achieved by advanced primary- or secondary-side modulation methods [4],[5]. On the other hand, regardless of the modulation method applied, these converters suffer from increased voltage stress across AC-side transistors due to resonance between the transformer leakage inductance and equivalent parasitic capacitance of the circuit elements. Various approaches have been reported to reduce the impact of these oscillations and to improve the converter performance. In [6], dissipative passive RC snubbers

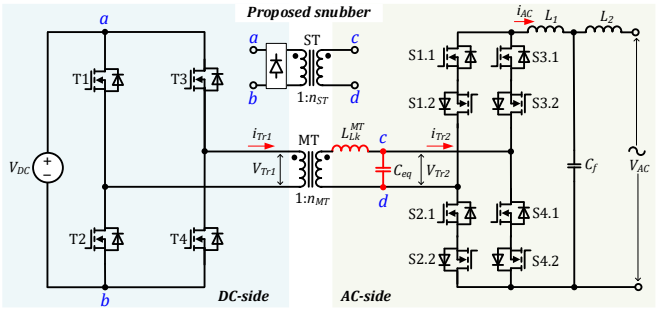

Fig. 1. Topology of the full-bridge HFLC.

TABLE I
Parameters and Components of the Experimental Prototype

Parameter	Symbol	Value
Input voltage	V_{CF}	350 VDC
Output voltage	V_{VF}	230 VAC
Switching frequency	f_{sw}	50 kHz
CF side inductor	L_1, L_2	1 mH, 0.3 mH
Main transformer turns ratio	n_{MT}	1.04
Snubber transformer turns ratio	n_{AT}	1.10
Rated power	P_{rated}	1 kW
CF Transistors	S_1-S_4	C3M0280090
VF Transistors	S_5-S_8	C3M0280090
Snubber diodes	D_1-D_4	HER158
Microcontroller	-	TMS320F28335

are applied across semiconductor devices to damp the oscillations. Despite its simplicity, such approach becomes less feasible at higher switching frequencies due to increased power dissipation. The active regenerative auxiliary circuit based on the flyback topology was proposed for primary-side modulated HFLC in [5]. It reduces the voltage overshoot and assists in operation with the non-unity power factor. Another version of the flyback snubber along with the extended dead-time approach was proposed for a secondary-side modulated converter in [7]. Despite mitigating the problem of voltage overshoot, such solutions are quite complex and require an additional multi-winding transformer, controlled semiconductors, isolated high-side drivers, and feedback loop, all rated for full voltage of the system [8]. A modified HFLC topology that applies two-step voltage on bridge semiconductors proposed in [9] showed promising results in terms of overshoot reduction and overall increase of the converter efficiency. However, the solution uses an extra switching leg, an additional transformer and needs to be rather precisely tuned to perform optimally. Another solution was described in [9], where a transformer with dynamic tapping was implemented to address the impact of varying input voltage on the overshoot amplitude.

This work was supported in part by the Estonian Centre of Excellence in Zero Energy and Resource Efficient Smart Buildings and Districts under Grant 2014-2020.4.01.15-0016 funded by the European Regional Development Fund, in part by the European Economic Area (EEA) and Norway Financial Mechanism 2014–2021 under Grant EMP474 and in part by the scientific project of Ministry of Science of Ukraine "Energy supply system for high-frequency drone reluctance switched motors with multi-cell converters and space-time modulation", № 0120U102131.

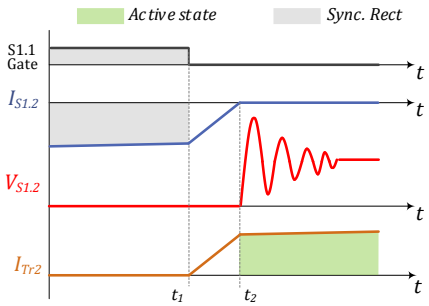

Fig. 2. Representation of the oscillation at the beginning of the HFLC active state: transistor S1.2 ends operating in the synchronous rectification mode.

It follows that the problem of voltage overshoots cannot be easily mitigated in the HFLCs that take advantage of the MOSFET technology and higher operating frequency. The overshoot reduction methods recently introduced are rather complex and may not offset the provided benefits due to additional components and corresponding cost increase.

This letter proposes a simple passive regenerative snubber that can be applied to HFLC topologies to mitigate the problem of overshoot and parasitic oscillations. The case study converter is described in Section II. Section III analyzes the proposed snubber circuit and its operation is verified in Section IV. Finally, the feasibility of the solution is addressed in the conclusions.

II. Full-Bridge High-Frequency Link Converter

The case study converter is based on the widely addressed topology consisting of a DC-side full bridge (FB) and AC-side FB composed of bidirectional switches (using two anti-series MOSFETs), separated by a two-winding isolation transformer (MT), as shown in Fig. 1. The main parameters of the case study converter are listed in Table I. The AC waveform is generated using the quasi-resonant phase-shift modulation applied to the secondary side transistors [11].

Similar to other soft-switching modulation methods, the overshoots and oscillations appear across the secondary AC side due to resonant ringing between transformer leakage inductance and device output capacitance (Fig. 2) [4]-[9]. The current and voltage during the resonance are described by

$$i_{ls}(t) = \left(i_0 \cdot \cos(\omega t) + \frac{n_{MT} \cdot V_{DC}}{\rho} \cdot \sin(\omega t) \right) \cdot e^{-T_{osc}/4 \cdot \tau_{Lk}}, \quad (1)$$

$$v_{Ceq}(t) = n_{MT} \cdot V_{DC} - \left(n_{MT} \cdot V_{DC} \cdot \cos(\omega t) + i_0 \cdot \rho \cdot \sin(\omega t) \right) \cdot e^{-T_{osc}/4 \cdot \tau_{Lk}}, \quad (2)$$

where i_0 is the initial leakage inductance current that takes into account the finite recovery time of a transistor's body diode; C_{eq} is the equivalent capacitance; L_{Lk}^{MT} is the equivalent leakage inductance of the MT referred to AC-side winding; ρ is the characteristic impedance $\rho = (L_{Lk}^{MT}/C_{eq})^{-0.5}$; ω is the resonant frequency $\omega = (L_{Lk}^{MT} \cdot C_{eq})^{-0.5}$; τ_{Lk} is the time constant reflecting the losses in the oscillatory circuit.

Neglecting the diode reverse recovery, for i_0=0, the peak voltage V_{Peak} can reach two times the steady-state voltage level, increasing to 2.4 times in case the reverse recovery current equal to the load current was initially flowing in the circuit. This can lead to an undesired avalanche effect or

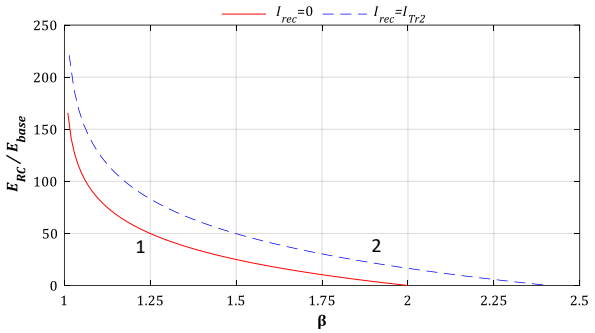

Fig. 3. Relation of the loss factor E_{RC} / E_{base} dependence on the relative voltage overshoot β.

increased voltage rating requirement for semiconductors. Due to the high number of devices at the AC-side, this generally results in poor silicone utilization, which is one of the major limits for a wider adoption of HFLC in practical applications, especially at higher power levels. The use of passive RC snubbers to reduce the voltage overshoots is generally ineffective, as they need to dissipate significant energy to reduce the voltage overshoot noticeably [8]. The energy dissipation of the RC-snubber E_{RC} for a given voltage overshoot β can be compared against the initial power in the oscillatory circuit P_{base}:

$$\frac{E_{RC}}{E_{base}} = \frac{36 \cdot \pi \cdot (n_{MT} \cdot V_{DC})^2 \ln\left(1/(\beta - 1)\right)}{t_{sp} \cdot \omega \cdot (V_{peak} - n_{MT} \cdot V_{DC})^2}, \quad (3)$$

where t_{sp} is the time instant of a first voltage peak:

$$t_{sp} = \begin{cases} \pi/\omega, & V_{peak} = 2 \cdot n_{MT} \cdot V_{DC}; \\ 3\pi/(4 \cdot \omega), & V_{peak} = 2.4 \cdot n_{MT} \cdot V_{DC}; \end{cases} \quad (4)$$

Fig. 3 depicts relative losses in the RC snubber for two cases:

1. neglecting the influence of reverse recovery current I_{rec} (V_{peak}=2·n_{MT}·V_{DC});
2. with initial I_{rec}=I_{Tr2} (V_{peak} = 2.4·n_{MT}·V_{DC}).

As shown, a reduction of overshoot down to 1.5·n_{MT}·V_{DC} would require to dissipate the amount of energy that is 25…50 higher than the one initially present in the oscillatory circuit, leading to significant losses and compromised efficiency of the converter.

III. Proposed Passive Regenerative Snubber

Operating principle

The proposed snubber is based on a transformer (ST) and a diode FB connected between the DC source and the secondary winding (Fig. 1).

The turns ratio of the ST is chosen such that $n_{MT} < n_{ST}$ (see Fig. 1 and Table I). In this case, the snubber circuit does not transfer active power in the steady-state converter operation mode and the equivalent circuit can be represented as shown in Fig. 4a. The snubber is activated only during an overshoot event, then the voltage across the C_{eq} rises above the steady-state value and the following criterion is satisfied:

$$V_{DC} < v_{Ceq} / n_{ST}. \quad (5)$$

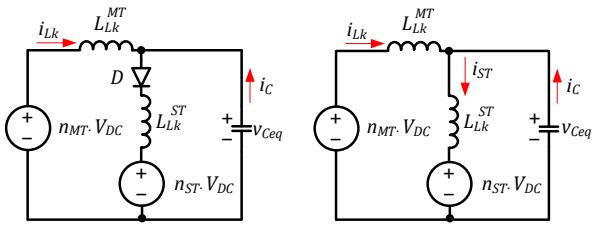

Fig. 4. Equivalent circuits describing the snubber operation: non-active mode (a) and regeneration mode (b).

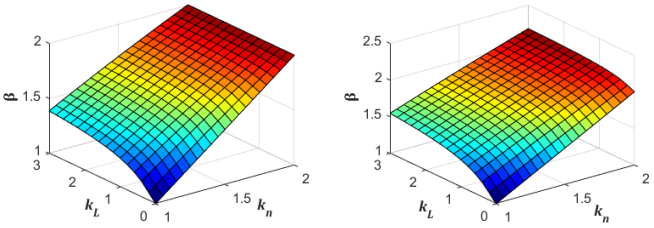

Fig. 5. Generalized dependencies between relative snubber transformer parameters k_L and k_n vs. the relative amplitude of voltage overshoot: (a) i_0=0, and (b) i_0=n_{MT}·V_{DC}/ρ; $e^{-T_{osc}/4\cdot\tau_{Lk}}=0.65$.

In this case, the equivalent circuit corresponds to that shown in Fig. 4b. In this mode, the equivalent inductance in the circuit becomes equal to:

$$L_{eq}=\frac{L_{Lk}^{MT}L_{Lk}^{ST}}{L_{Lk}^{MT}+L_{Lk}^{ST}}=L_{Lk}^{MT}\frac{k_L}{1+k_L}, \quad (6)$$

where L_{Lk}^{ST} is the equivalent leakage inductance of the ST referred to the AC-side winding $k_L=L_{Lk}^{ST}/L_{Lk}^{MT}$. As a result, the angular frequency ω is increased to ω' and the time constant decreases accordingly:

$$\tau'_{Lk}=\frac{\omega}{\omega'}\cdot\tau_{Lk}, \quad (7)$$

where $\omega'=1/\sqrt{L_{eq}\cdot C_{eq}}$.

$$\beta=\frac{V_{Peak(sn)}}{n_{MT}\cdot V_{DC}}=\begin{cases}k_n+\left(\left(1-(k_n-1)^2\right)\cdot\sqrt{\dfrac{k_L}{1+k_L}}+k_n(k_n-1)+\dfrac{k_L+k_n}{1+k_L}(2-k_n)-k_n\right)e^{-T_{osc}/4\cdot\tau'_{Lk}}, & i_0=0;\\ k_n+\left(\left(1-\dfrac{(k_n-1)^2}{2}\right)\cdot\sqrt{\dfrac{2k_L}{1+k_L}}+k_n\dfrac{k_n-1}{\sqrt{2}}+\dfrac{k_L+k_n}{1+k_L}\left(1-\dfrac{k_n-1}{\sqrt{2}}\right)-k_n\right)e^{-T_{osc}/4\cdot\tau'_{Lk}}, & i_0=\dfrac{n_{MT}\cdot V_{DC}}{\rho},\end{cases} \quad (8)$$

where: $k_n=n_{ST}/n_{MT}$; $\rho'=\sqrt{L_{eq}/C_{eq}}$; $T_{osc}=2\pi\cdot\sqrt{L_{eq}\cdot C_{eq}}$

Design guidelines

In a general case, a preferable ST design is based on a core smaller than that of MT, with a smaller wire cross-section and a higher number of turns. In the case of an ideal ST, the maximum current at the second winding is

$$I_{\max}^{ST}=\sqrt{C_{eq}\cdot\left(\left(V_{Pk}-n_{MT}\cdot V_{DC}\right)^2-\left(n_{ST}\cdot V_{DC}\right)^2\right)/L_{Lk}^{MT}}. \quad (9)$$

From the maximum value, this current starts to decay to zero during the following interval:

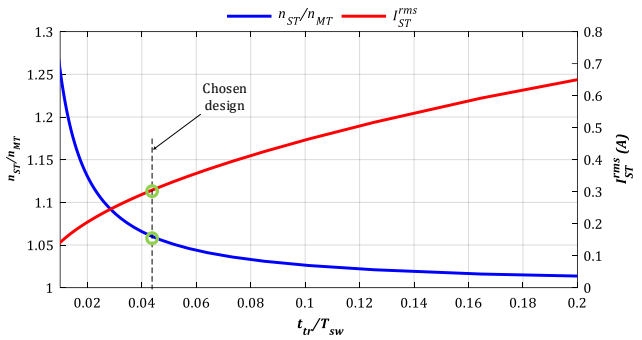

Fig. 6. Trade-off between various snubber transformer parameters.

TABLE II
PARAMETERS OF THE MAIN AND SNUBBER TRANSFORMERS

Parameter	MT	ST
Core, material	ETD59, 3C97	36/23/10, 3C94
Magnetizing inductance (L_m)	12.8 mH	32.8 mH
Turns ratio	46/44	128/116
Winding material	0.2×60 litz wire	Copper wire AWG23
DC resistance, primary	0.135 Ω	1.02 Ω
DC resistance, secondary	0.16 Ω	1.25 Ω
Leakage inductance (L_{Lk})	15μH	5.1 μH
Isolation	Polyimide tape 0.076mm (6 kV)	

Part of the energy that is present in the oscillatory circuit is regenerated back to the input source and the initial V_{Peak} value is reduced to $V_{Peak(sn)}$. The relative voltage overshoot can be estimated by (8). As can be seen, the amount of overshoot reduction is closely related to the parameters of the ST. The dependencies are plotted in Fig. 5. In the practical systems, the parameter n_{ST}/n_{MT} should be in the range 1.05…1.2 to prevent regeneration of the non-oscillatory energy and to obtain good trade-off between the voltage overshoot reduction, duration of the regeneration interval and rms current in the snubber.

$$t_{tr}=\frac{\sqrt{L_{Lk}^{MT}\cdot C_{eq}\left(\left(V_{Pk}-n_{MT}\cdot V_{DC}\right)^2-\left(n_{ST}\cdot V_{DC}\right)^2\right)}}{n_{MT}\cdot V_{DC}\cdot(k_n-1)}, \quad (10)$$

Considering four regeneration intervals per switching period, the corresponding rms current of ST is

$$I_{ST}^{rms}=I_{ST}^{\max}\sqrt{4\cdot t_{tr}/3T_{sw}}, \quad (11)$$

The turns ratio of the ST can be chosen according to the characteristics in Fig. 6, which was obtained using (10) and (11). For the current study, n_{ST}=1.1 (which assumes n_{ST}/n_{MT} = 1.057) was selected to keep the total power transferred by the snubber around 10% of the converter rated power and ensure

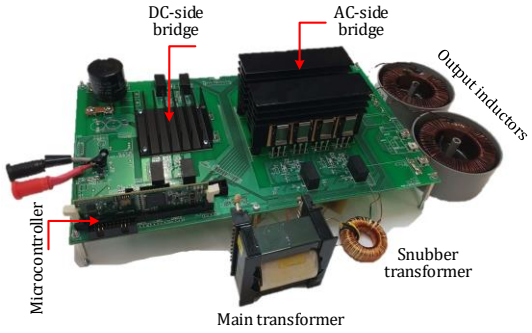

Fig. 7. Photo of the experimental HFLC prototype.

that the regeneration time is within 5% of the switching period. The design of the ST based on a compact toroid core was selected. The parameters of the MT and ST are listed in Table II. The diodes for the FB rectifier have to be selected in accordance with voltage and current requirements. In the current implementation, ultrafast Si diodes were used (see Table I), while for higher frequencies, SiC Schottky diodes can be more preferable due to lower switching losses.

IV. Experimental Verification

The proposed snubber was verified using the experimental HFLC (Fig. 7), with parameters and components listed in Tables I and II. The converter was operating in the DC-AC mode with open-loop control on a resistive load. A series of experiments with different snubber configurations were performed to evaluate their influence on the peak voltage overshoot and the overall converter efficiency. The general switching waveforms are demonstrated in Fig. 8a and the oscillations that occur in the AC-side are shown in Fig. 8b. As observed, the amplitude of the first voltage overshoot can exceed 800 V (Fig. 9a). This forces one to utilize 900 V or higher class MOSFETs to avoid the avalanche effect. In the frame of our sets of experiments, the addition of various RC snubbers connected between "c" and "d" points in Fig. 1 resulted in the reduction of the overshoot down to 630 V for about 12 W power dissipation (Fig. 9b) and further decrease of overvoltage by means of an RC snubber was considered infeasible.

The operation of the proposed snubber is demonstrated in Fig. 8c. As can be seen, the snubber is activated two times throughout the converter switching half-period. During the regeneration interval, the oscillation frequency increases due to the reduction of resonant circuit inductance owing to the parallel operation of both MT and ST, as estimated by (4) and (5) (Fig. 9c). The power regenerated by the snubber was around 110 W, providing peak overshoot reduction down to 560 V.

Finally, the combination of a regenerative and an RC snubber was tested to evaluate the impact on further overshoot reduction and efficiency. The experimental results at rated power for different configurations are summarized in Fig. 10. The efficiencies for different operating power levels are presented in Fig. 11. The RC snubbers were implemented with varying capacitance value, while the resistance R_{sn} was kept at 50 Ω. It is evident that for the case study system, the reduction of the overshoot using only an RC snubber has marginal feasibility due to efficiency reduction, which is becoming even more pronounced at part-load operation. On the other hand, the proposed snubber achieves significant overshoot reduction, without noticeably affecting the efficiency. Finally, the combined snubber achieves superior overshoot reduction for the same efficiency cost when compared to the single RC snubber. The overshoot below 500 V was obtained with around 12 W power dissipation.

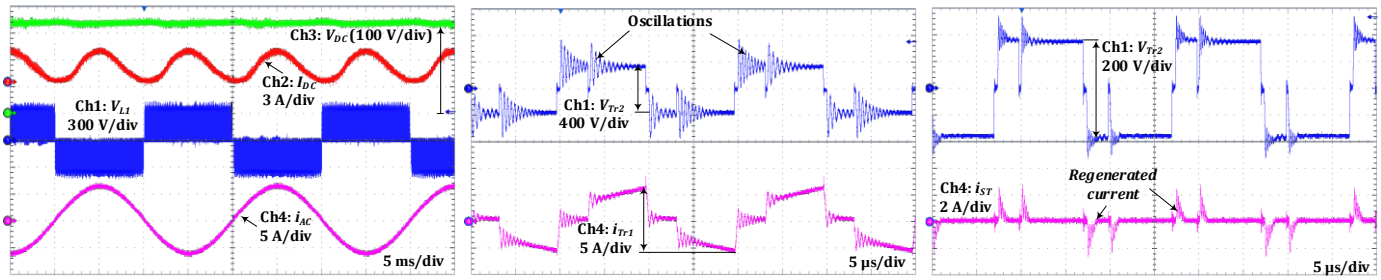

(a) (b) (c)

Fig. 8. General input/output waveforms of the HFLC (a), MT AC-side voltage and current – without snubber (b) and ST AC-side voltage and current (c).

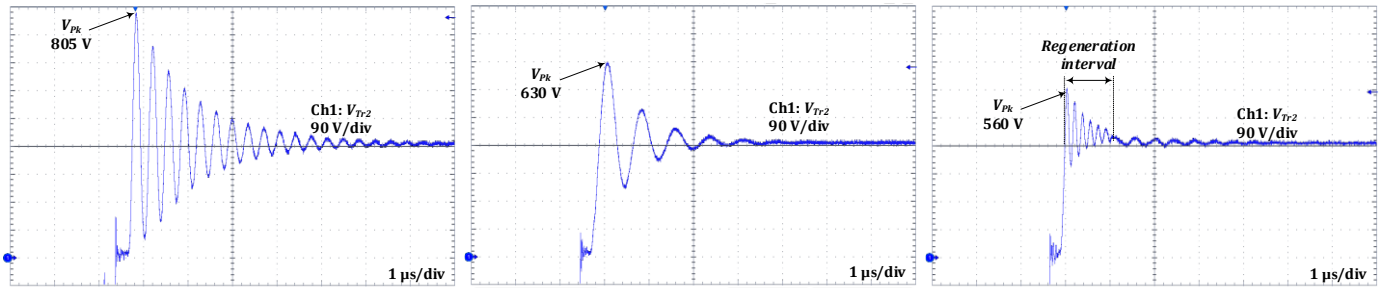

(a) (b) (c)

Fig. 9. Voltage overshoot in the AC-side of the HFLC: basic circuit (a), RC snubber (630 pF, 50 Ω) (b) and proposed regenerative snubber (c).

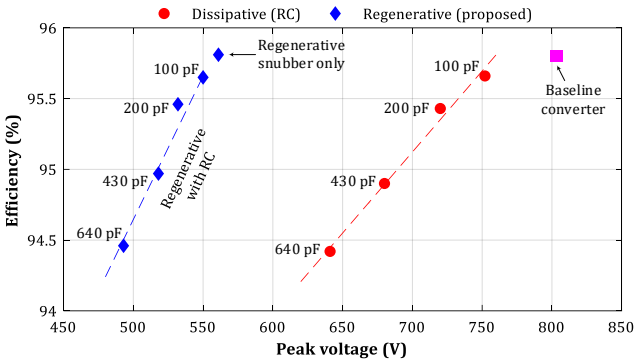

Fig. 10. Measured efficiency and peak voltage overshoots obtained with different snubber configurations at 1 kW (R_{sn}=50 Ω).

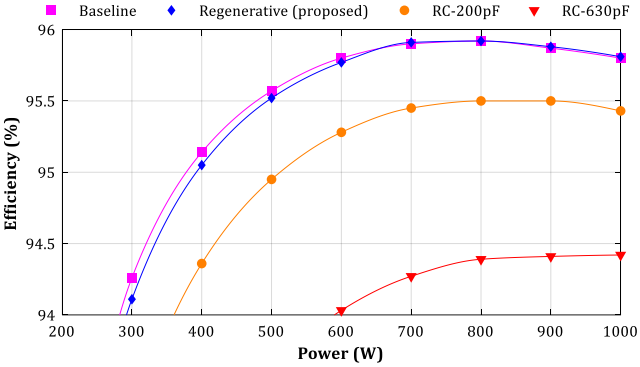

Fig. 11. Measured efficiency vs. power with different snubber configurations (R_{sn}=50 Ω).

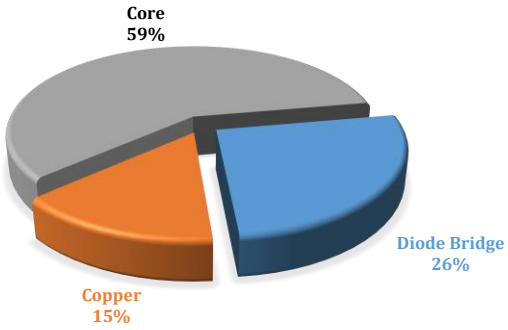

Fig. 12. Power loss breakdown of the proposed regenerative snubber circuit ($P_{sn(total)}$=4.0 W).

The power loss breakdown of the proposed snubber circuit is presented in Fig. 12. As shown, most of the losses are occurring in the core. Still, for 110 W of regenerated power, the efficiency of the snubber is estimated at around 96.4%. If necessary, this value can be still improved by further optimizations in the transformer design.

V. Discussion and Conclusions

This letter presented a simple regenerative passive snubber for the reduction of voltage overshoots at the AC-side of the HFLC. Due to the presence of overshoots, voltage overrated semiconductor devices typically have to be used in the basic topology to avoid their avalanche breakdown. While this can be tolerated for low power, for higher power converters, the introduction of certain overshoot reduction techniques is favored to reduce the overall semiconductor VA rating. While some of the existing clamping methods [7]-[9] demonstrate even more significant overshoot reduction than that of the snubber proposed, they generally involve actively controlled circuits or substantial topology modifications and complexity increase, which can be generally justified for higher power systems due to significant semiconductor costs [11].

The proposed snubber enables the use of 650 V class semiconductor devices instead of 900 V at the AC-side of the topology (assuming around 100 V safety margin), without negative effect on the overall efficiency. Further overvoltage reduction is possible using the combination with an RC snubber, when lower voltage requirements need to be achieved. Since the circuit is completely passive, it adds little complexity and component count, which is an advantage in applications where the effect provided by the snubber can be considered sufficient.

References

[1] D. Kumar, F. Zare and A. Ghosh, "DC Microgrid Technology: System Architectures, AC Grid Interfaces, Grounding Schemes, Power Quality, Communication Networks, Applications, and Standardizations Aspects," in *IEEE Access*, vol. 5, pp. 12230-12256, 2017.

[2] Yaosuo Xue, Liuchen Chang, Sren Baekhj Kjaer, J. Bordonau and T. Shimizu, "Topologies of single-phase inverters for small distributed power generators: an overview," in *IEEE Trans. Power Electron*., vol. 19, no. 5, pp. 1305-1314, Sept. 2004.

[3] O. Korkh, A. Blinov, D. Vinnikov, and A. Chub, "Review of Isolated Matrix Inverters: Topologies, Modulation Methods and Applications," *Energies*, vol. 13, no. 9, p. 2394, May 2020.

[4] Wang, M.; Guo, S.; Huang, Q.; Yu, W.; Huang, A.Q. An Isolated Bidirectional Single-Stage DC–AC Converter Using Wide-Band-Gap Devices With a Novel Carrier-Based Unipolar Modulation Technique Under Synchronous Rectification. *IEEE Trans. Power Electron*. 2017, 32, 1832–1843.

[5] Nayak, P.; Rajashekara, K.; Pramanick, S. Soft-Switched Modulation Technique for a Single-Stage Matrix-Type Isolated DC–AC Converter. *IEEE Trans. Ind. Appl*. 2019, 55, 7642–7656.

[6] Norrga, S. Experimental Study of a Soft-Switched Isolated Bidirectional AC DC Converter Without Auxiliary Circuit. *IEEE Trans. Power Electron*. 2006, 21, 1580–1587.

[7] Kummari, N.; Chakraborty, S.; Chattopadhyay, S. An Isolated High-Frequency Link Microinverter Operated with Secondary-Side Modulation for Efficiency Improvement. *IEEE Trans. Power Electron*. 2018, 33, 2187–2200.

[8] Korkh, O.; Blinov, A.; Vinnikov, D. Analysis of Oscillation Suppression Methods in the AC–AC Stage of High Frequency Link Converters. In Proceedings of the 2019 IEEE 60th International Scientific Conference on Power and Electrical Engineering of Riga Technical University (RTUCON), Riga, Latvia, 7–9 October 2019; pp. 1–5.

[9] N. Kummari and S. Chattopadhyay, "Three-Legged High-Gain Phase-Modulated DC–AC Converter for Mitigation of Device Capacitance Induced Ringing Voltage," in *IEEE Trans. Power Electron*., vol. 35, no. 2, pp. 1306-1321, Feb. 2020

[10] S. K. Mazumder, R. K. Burra, R. Huang, M. Tahir and K. Acharya, "A Universal Grid-Connected Fuel-Cell Inverter for Residential Application," in *IEEE Trans. Ind. Electron.*, vol. 57, no. 10, pp. 3431-3447, Oct. 2010,

[11] A. Blinov, O. Korkh, D. Vinnikov, I. Galkin and S. Norrga, "Soft-Switching Modulation Method for Full-Bridge DC-AC HF-Link Inverter," IECON 2019 - 45th Annual Conference of the IEEE Industrial Electronics Society, Lisbon, Portugal, 2019, pp. 4417-4422.

[12] T. Kjellqvist, S. Ostlund and S. Norrga, "Active Snubber Circuit for Source Commutated Converters Utilizing the IGBT in the Linear Region," in *IEEE Trans. on Power Electron*., vol. 23, no. 5, pp. 2595-2601, Sept. 2008